www.sciencemag.org/cgi/content/full/science.1233029/DC1

Supplementary Materials for

Sept4/ARTS Regulates Stem Cell Apoptosis and Skin Regeneration

Yaron Fuchs, Samara Brown, Travis Gorenc, Joe Rodriguez, Elaine Fuchs,* Hermann Steller*

*Corresponding author. E-mail: steller@rockefeller.edu (H.S.); fuchslb@rockefeller.edu (E.F.)

Published 20 June 2013 on *Science* Express
DOI: 10.1126/science.1233029

This PDF file includes:

Materials and methods

Mice

Sept4/ARTS$^{-/-}$, XIAP$^{-/-}$ and XIAP$^{\Delta RING}$ were described previously (*7, 25, 32*). *Tg(Krt1-15-EGFP)2Cot/J, Tg(Krt1-15-cre/PGR)22Cot* and *Rosa26-YFP* mice were purchased from Jackson.

Flow cytometry

HFSC isolation and FACS analysis was performed with K15-GFP and CD34, Integrin α6, Integrin β1 and Sca1 antibodies as previously described (*33, 34*). HFSCs as well as Sca-I^{+} keratinocytes were isolated from the backskin of 8-week-old mice (telogen).

Histology and Immunofluorescence

Skins were embedded in OCT, frozen, sectioned, and fixed in 4% formaldehyde. For paraffin sections, skins were incubated in 4% formaldehyde at 4°C overnight, dehydrated with a series of increasing concentrations of ethanol and xylene, and embedded in paraffin. Paraffin sections were rehydrated using W-CAP (Bio-optica) and subjected to immunofluorescence microscopy. For immunohistochemistry, sections were subjected to antigen unmasking in 10 mM Citrate, pH 6.0. Sections were incubated with HRP conjugate secondary antibodies (Abs) followed by the HRP substrate, diaminobenzidine. Antibodies and dilutions are included in Supplemental Data. Tail samples of hair follicles were treated with 5mM EDTA for 4 hours at 37^{0}C to separate skin epithelium from dermis and fixed in formal saline for 2 hours in room temperature. DWMs were performed as in (*35*).

RT-PCR analysis

RT-PCR was performed using Express SYBR greener (Invitrogen). *Sept4* primers were previously described in (*12*).

Bulge stem cell culture, cell number and apoptosis assays

CD34^{+} bulge cells were isolated and cultured on mitomycin C-treated J2 3T3 fibroblasts. For assessing cellular expansion 10^{4} freshly isolated cells were plated into 35-mm plates. The numbers of colonies (>4 cells) and cell number counted two weeks post plating. For apoptotic

assays, $CD34^+$ bulge cells were plated on fibronectin coated cover slips in transwell in which the upper portion contains the J2 3T3 feeders. Transwells were utilized in order to sustain and easily monitor the $CD34^+$ cells prior to apoptotic stimuli. Two days post plating STS (1μM) and Eto (50 μM) were added for 2 hours or 14 hours, respectively. Cells were then fixed with 4% PFA and subjected to Immunofluorescence microscopy.

Wound repair and Cre induction

For all wound repair experiments, mice were sedated with ketamine/xylazine (5μg/g) administered by intraperitoneal injection. Mice were shaved and excision wounds were performed by punch biopsy extraction of $1cm^2$ dorsal-skin. PWI, mice were individually housed. At the desired time PWI, mice were euthanized with CO_2 and the wounded skins were harvested and placed in 4% paraformaldehyde for paraffin embedding or OCT. Cre^{PGR} was induced by topical application of RU486 (1% Sigma) dissolved in ethanol for 5 consecutive days.

Statistical analyses

All quantification data are mean ±SD. The significance of quantitative data was tested employing student T test.

Antibody Information

ARTS (Rabbit, 1:100, Sigma), CD34 (Rat, 1:100, ebioscience), K15 (Mouse, 1:100, Thermo, Chicken, 1:1000, Abcam), Sox9 (Rabbit, 1:100, Millipore, Goat, 1:50, Santa Cruz), Lgr6 (Rabbit, 1:200, Novus), Integrin α6 (Rat, 1:400, ebioscience), Integrin β1 (Hamster, 1:400, ebioscience), Sca1 (Mouse, 1:200, ebioscience), Cleaved-Caspase-3 (Rabbit, 1:100, Cell signaling), Cleaved-Caspase-7 (Rabbit, 1:100, Cell signaling), Cleaved-Caspase-9 (Rabbit, 1:100, Cell signaling), NFATc1 (Mouse, 1:100, Santa Cruz, Rabbit, 1:50, Abcam), TBX1 (Rabbit, 1:50, Abcam) PCNA (Rabbit, 1:100, Santa Cruz, Mouse, 1:100, Novus), Ki67 (Rabbit, 1:1000, Abcam), XIAP (Rabbit, 1:100, Santa Cruz), Lhx2 (Goat, 1:100, Santa Cruz), Tcf3 (Rabbit, 1:100, Santa Cruz, Rabbit, 1:100, Novus). TUNEL was performed using ApopTag TdT (Millipore).

Supplementary Figures

Figure S1. ARTS is expressed in the skin and regulates the number of HFSCs. A Left panel. Immunofluorescence (IF) of telogen-phase (P20) skin sections with ARTS, CD34 and K15 antibodies. **A Right panel.** IF on TWM indicating ARTS antibody specificity **B**. Anti-ARTS immunohistochemistry (IHC) of anagen-phase (P14) HFs from WT and *Sept4*/ARTS$^{-/-}$ mice. Immunolabeling for ARTS was detected in HFSCs, the HG, and the ORS cells of anagenic HFs. **C**. RT-PCR analysis of *Sept4* transcripts expressed in CD34^{+} HFSCs. HFSC *Sept4* expression levels were normalized to brain transcripts (top) and examined by gel electrophoresis (bottom). Lanes: CD34^{+}ScaI^{-} HFSCs (1), Brain (2), *Sept4*/ARTS$^{-/-}$ CD34^{+}ScaI^{-} HFSCs (3) and no template control (4). ARTS was the only *Sept4* transcript detectable in HFSCs indicating that it is the predominant if not the only splice variant expressed in these cells. **D**. Cells were first sorted for $\alpha6^{+}\beta1^{+}$ and then resorted for CD34^{+}Sca1^{-}.The percentage of CD34^{+}Sca1^{-} HFSCs was calculated from the $\alpha6^{+}\beta1^{+}$ population. Depicted is the percentage of CD34$^{+}\alpha6^{hi}$ and CD34$^{+}\alpha6^{low}$ cells. Average of WT CD34^{+}Sca1^{-} HFSCs is 6.04±1.9% and *Sept4*/ARTS$^{-/-}$ 12.65%±2.47% ($n\geq11$, $P<0.001$). Scale Bars: 10μm (B), 20μm (A Left), 200μm (A Right).

Figure S2. *Sept4*/ARTS$^{-/-}$ mice display an increased number of HFSCs. A, B. Percentage of HFs with extended ES **(A**) and length of bulge length and epithelial stand (**B**). **C, D**. Z-stack of whole mount telogen phase tailskins stained for HFSC markers K15 (**C**) and CD34 (**D**) (8-week-old mice). Scale Bars: 200μm. *** Indicates $P<0.001$.

Figure S3. *Sept4*/ARTS does not affect proliferation. A-D. Number of colonies (>4 cells) and fold increase of CD34^{+}Sca1^{-} HFSCs and CD34^{-}Sca1^{+} epidermal keratinocytes plated. Data are representative of three independent experiments. **E-G**. *Sept4*/ARTS does not affect proliferation *in vivo*. Quantification of the number of Ki67^{+} bulge cells (**E**), Ki67^{+}/K15^{+} epidermal cells (**F**) and proliferation in different skin compartments (**G**) (P21). **H**. Confocal DHW images of proliferating cells in the different skin compartments (P21). INF denotes infundibulum and IFE-interfollicular epidermis **I-K**. *Sept4*/ARTS does not affect proliferation *in vitro*. **I.** Confocal image of Ki67^{+} and control non-proliferating CD34^{+} cells. **J, K.** Quantification of the number of Ki67^{+} (**J**) and PCNA^{+} (**K**) CD34^{+} cells. Scale Bars: 5μm (I) 50μm (H). *** Indicates $P<0.001$.

Figure S4. *Sept4*/ARTS$^{-/-}$ HFSCs are resistant to apoptosis. A. Schematic of the new bulge (NB), old bulge (OB), hair germ (HG) and dermal papilla (DP) during second telogen. **B.** IF on dorsal whole mounts (P50) indicating that *Sept4*/ARTS$^{-/-}$ HFs form two bulges as WT mice do. **B. right panel**. Analyses of the numbers of K15-GFP^{+} HFSCs within the old and new bulges of WT and *Sept4*/ARTS$^{-/-}$ HFs. **C.** Percentage of HFs that encompass K15^{+}/CP3^{+} cells (P16). Outside the bulge, ~75% of WT HFs had at least one K15^{+}/CP3^{+} cell in the upper/mid ORS while *Sept4*/ARTS$^{-/-}$ HFs showed staining in only 1-2%. **D.** Immunofluorescence staining of dorsalskin HFs, demonstrating K15^{+}/CP3^{+} and K15^{+}/Sox9^{+}/TUNEL^{+} cells (P16). The data shown in B and C indicate that loss of *Sept4*/ARTS causes a striking decrease in apoptosis. **E. upper panels**. Immunofluorescence staining of tailskin HFs, demonstrating that deletion of *Sept4*/ARTS causes increased resistance of bulge cells towards apoptosis. **E lower panel left**. CP3^{+} cells are TUNEL positive. **E lower panel right.** Enlargement of apoptotic HFSCs, demonstrating apoptotic morphology such as membrane blebbing. Scale Bars: 5μm (E lower panels), 20μm (B, D) and 100μm (E upper panels) *** Indicates P<0.001.

Figure S5. CD34^{+} HFSCs can be grown without sustaining feeders. *Sept4*/ARTS$^{-/-}$ and control CD34^{+} HFSCs were grown without sustaining J2 feeder cells on either fibronectin- or collagen-coated plates. **A**. Bright field photographs of cells two weeks post plating. **B**. Fold increase in CD34^{+} cell number of cells plated on fibronectin coated plates. *Sept4*/ARTS$^{-/-}$ HFSCs reached confluence under conditions that severely hindered the growth of control cells, indicating that they are protected from stress in the absence of feeder cells. Scale bar indicates 500μm. *** Indicates P>0.001

Figure S6. Loss of *Sept4*/ARTS function accelerates wound healing and improves skin regeneration. **A**. Pictures of 8-week-old mice, 5 days PWI. Dashed line represents wound border. **B**. Immunofluorescence for PCNA, indicating proliferative activity within the regenerated HF niche in *Sept4*/ARTS$^{-/-}$ mice. Proliferating cells were predominantly positioned along the leading edge of regenerating HFs and, in this regard, resembled WT HFs (*18*). Scale Bar: 10μm.

Figure S7. An increased number of YFP^{+} cells in the hair follicle and wounded epidermis of

***Sept4*/ARTS$^{-/-}$ mice.** Reporter expression was induced in *Tg(Krt1-15-cre/PGR)22Cot;*Rosa26-YFP; *Sept4*/ARTS$^{-/-}$ and control mice for 5 consecutive days with RU486 from P20-P25 or P45-P50, and wounding was executed at P26 or P56. Skins were analyzed for YFP with/without HFSC markers at t=0d (**A, B**), 7d (**C, D**) and 18d-PWI (**E, F**). **G**. Zoom-in on regenerated HF in *Sept4*/ARTS$^{-/-}$ mice 18d-PWI. Dashed line indicates dermis-epidermis border. Eighteen days PWI, both regenerated HFs and sebaceous glands in the wound bed of P74 *Sept4*/ARTS$^{-/-}$ skins still displayed YFP^{+} cells. Scale Bars: 20 μm (A, B, E), 50 μm (G) 100μm (C, D, F).

Figure S8. XIAP is expressed primarily in the HFSC niche, dermal papilla and sebaceous gland. A. IF staining employing XIAP antibody was performed on skin section excised from the back K15-GFP reporter mice (P14) **B**. XIAP expression in the dermal papilla (DP; P14). **C**. During telogen (P20) XIAP can be witnessed in the HFSC niche as well as in the sebaceous gland. Scale Bar: 200μm (A) and 50μm (B,C).

Figure S9. Figure S8. XIAP is regulated by and epistatic to *Sept4/ARTS*.
A. Western blot demonstrating increased XIAP protein levels in *Sept4*/ARTS$^{-/-}$ HFSCs. Densitometry was performed using GelquantNET software **B.** H&E staining of full thickness excision wounds inflicted on 15-week old male mice. Seven days PWI, mice were euthanized and wounds were harvested. Arrows indicate regenerated HFs. Dashed line indicates dermis-neoepidermis border. Denotation: NE- neoepidermis and GT- wound granulation tissue. Scale Bar: 100μm.

Figure S10. Deletion of XIAP suppresses *Sept4/ARTS* phenotypes in the skin and affects HFSC apoptosis. A. Survival of *Sept4*/ARTS$^{-/-}$ CD34^{+} HFSCs is mediated by XIAP and its RING domain. WT, *Sept4*/ARTS$^{-/-}$, XIAP$^{-/-}$, SX$^{-/-}$ and SX$^{\Delta Ring}$ CD34^{+} HFSCs were grown without sustaining J2 feeder cells on fibronectin-covered plates. In contrast to *Sept4*/ARTS$^{-/-}$ HFSCs, which exhibited a dramatic increase in cell number, the growth of SX$^{-/-}$ and SX$^{\Delta RING}$ SCs was impaired even more severely than the growth of WT control cells. **A**. Bright field photographs of cells two weeks post plating. **B**. Fold increase in (CD34^{+} plated) cell number. **C, D** IF of (CD34^{+} plated) HFSCs for cleaved-caspase 7 (CP7, **C**) and cleaved-caspase 9 (CP9, **D**) demonstrating decreased number in *Sept4*/ARTS$^{-/-}$ and increased number in XIAP$^{-/-}$ HFSCs.

Scale Bar: 500µm. (*** Indicates P>0.001).

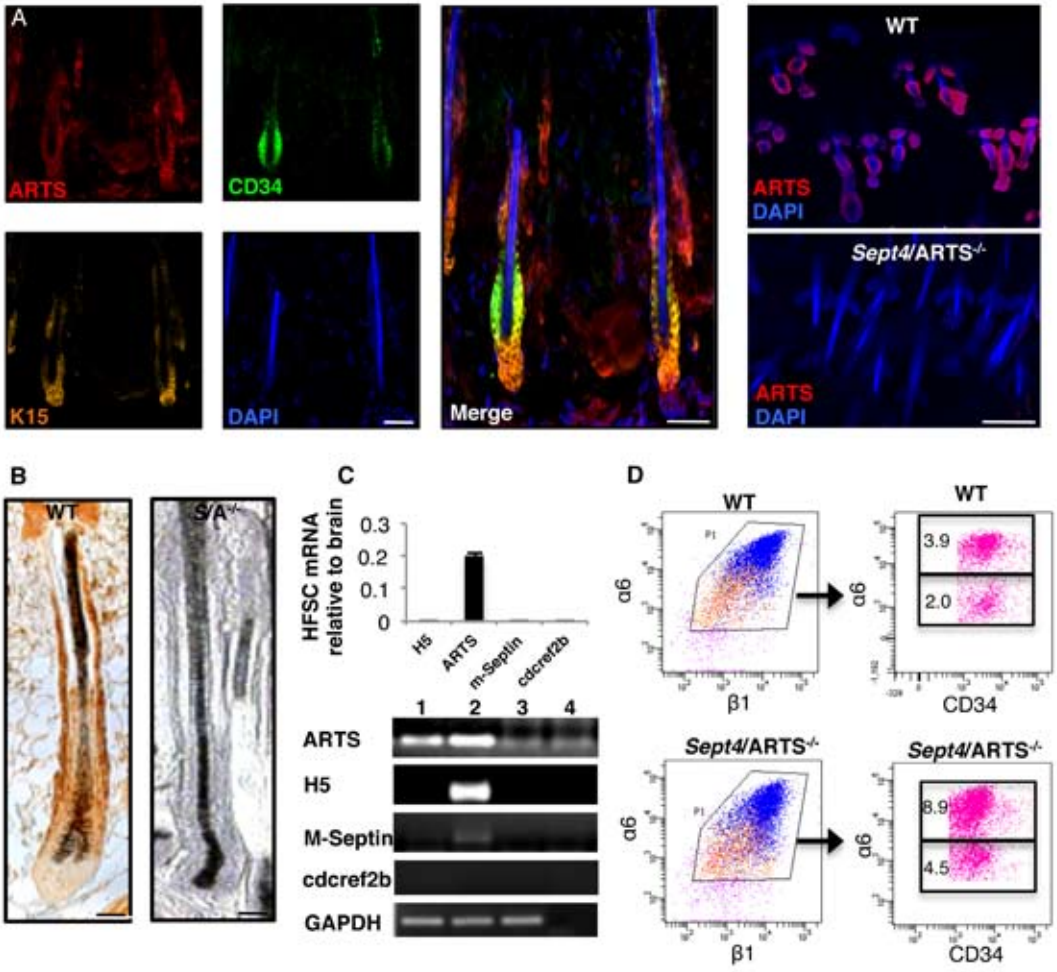

Figure S1. ARTS is expressed in the skin and regulates the number of HFSCs.

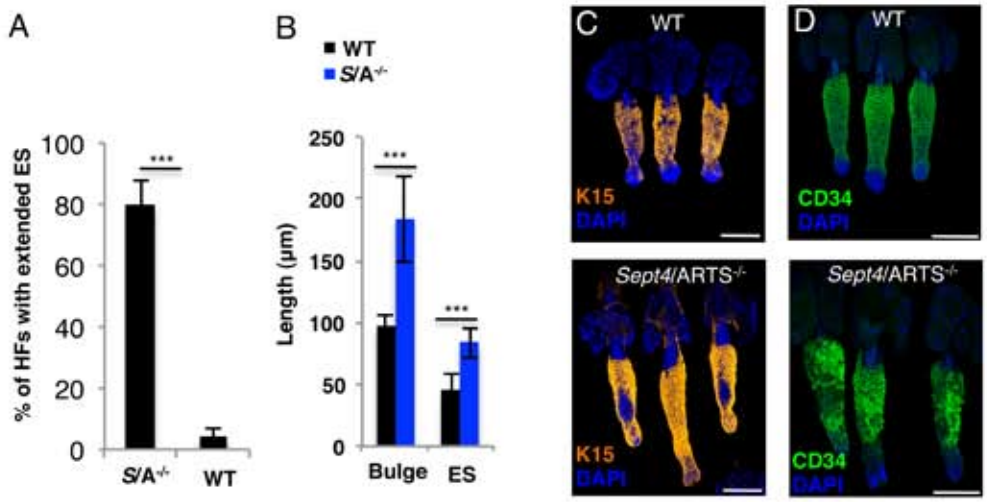

Figure S2. *Sept4*/ARTS$^{-/-}$ mice display increased bulge and ES size.

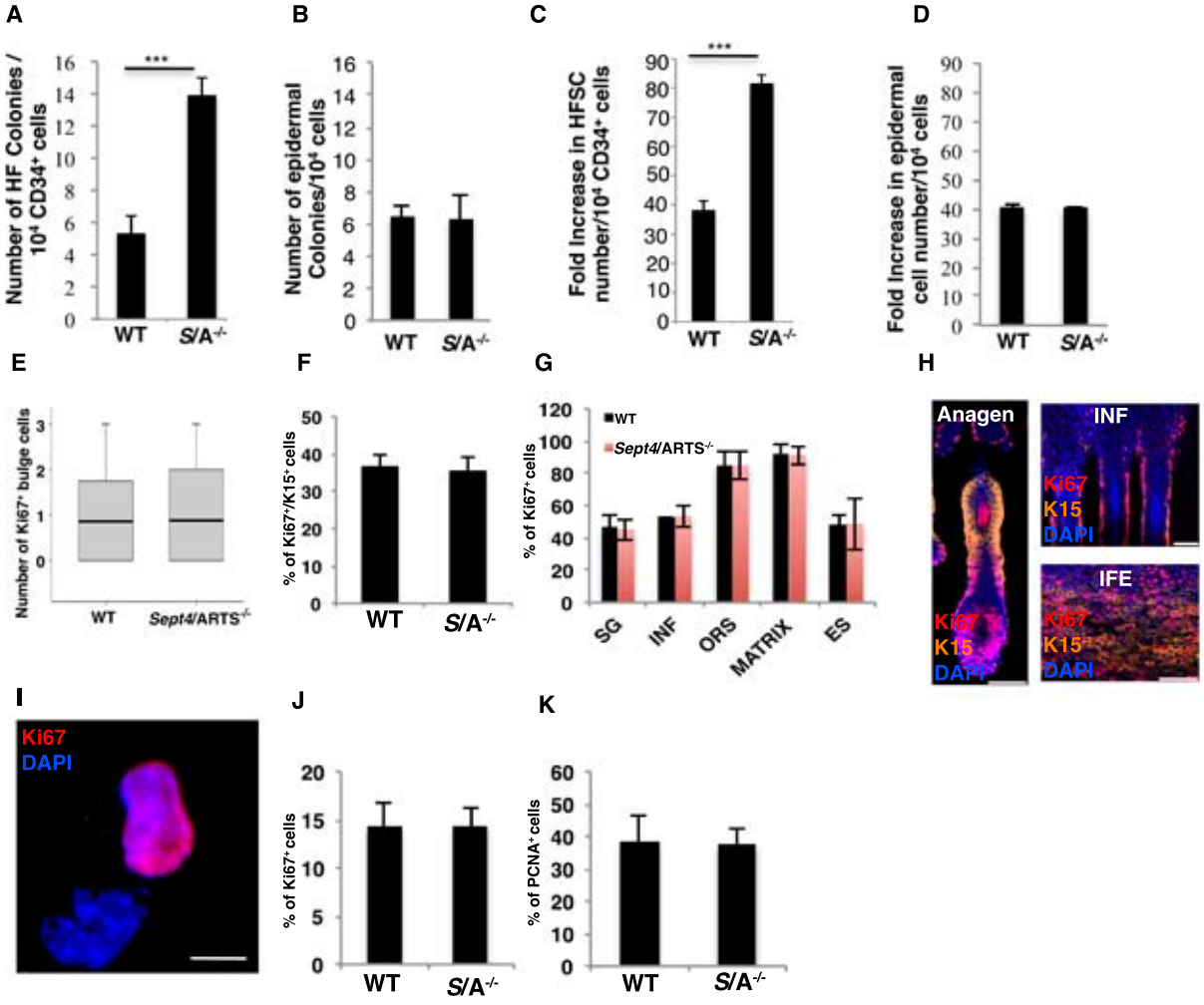

Figure S3. *Sept4*/ARTS does not affect proliferation.

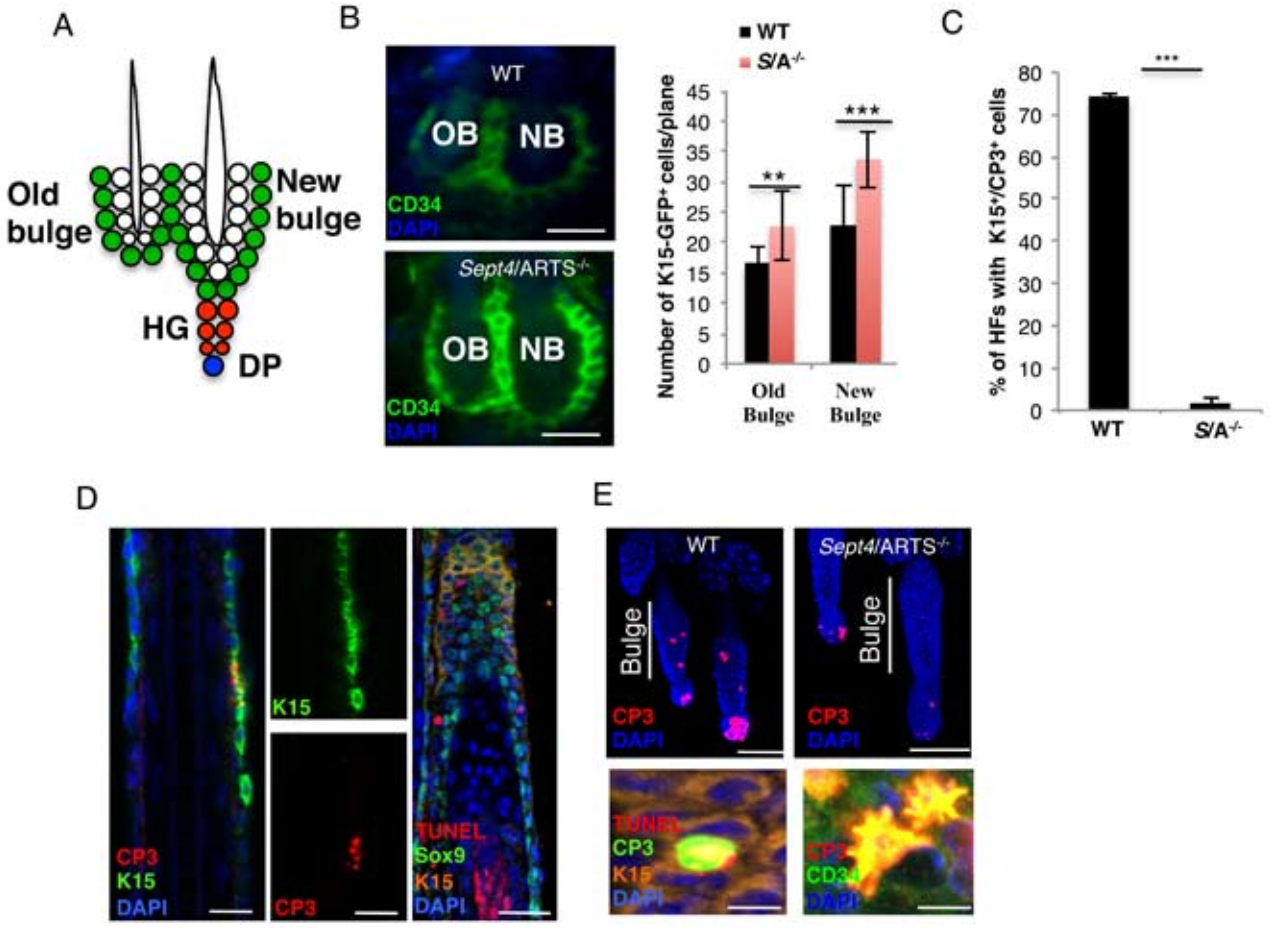

Figure S4. *Sept4*/ARTS$^{-/-}$ HFSCs are resistant to apoptosis.

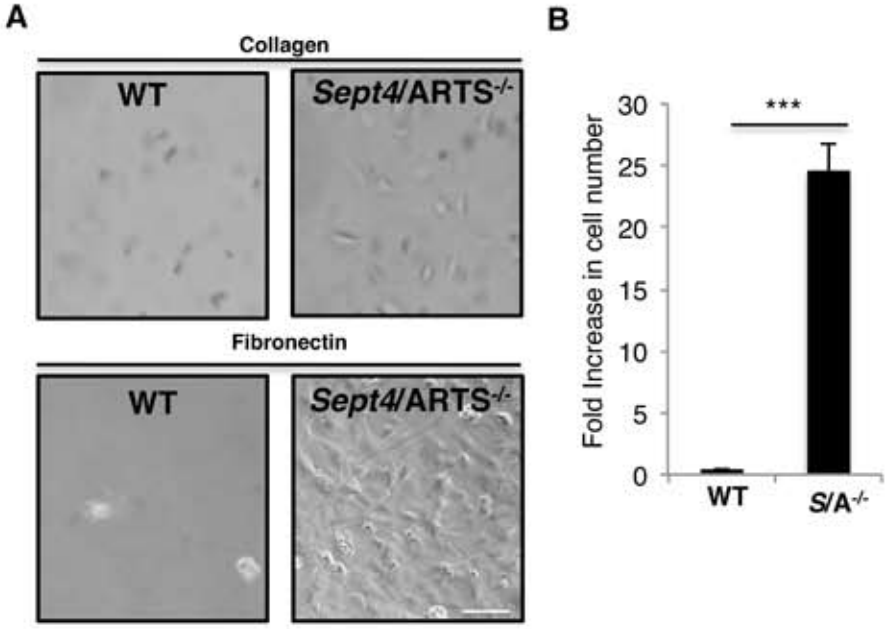

Figure S5. CD34⁺ HFSCs can be grown without sustaining feeders.

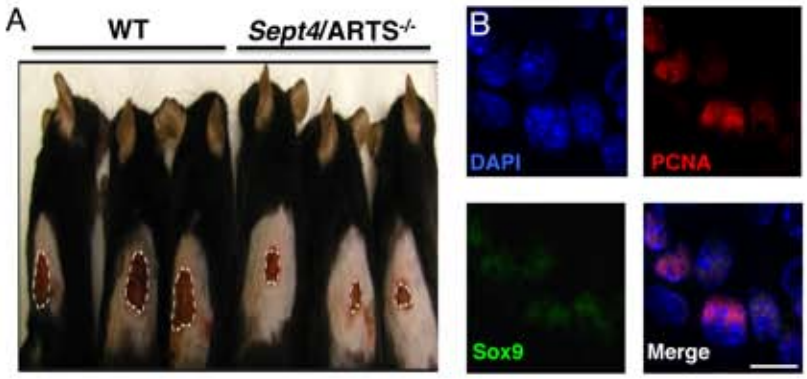

Figure S6. Loss of *Sept4*/ARTS function accelerates wound healing and improves regeneration of HFs.

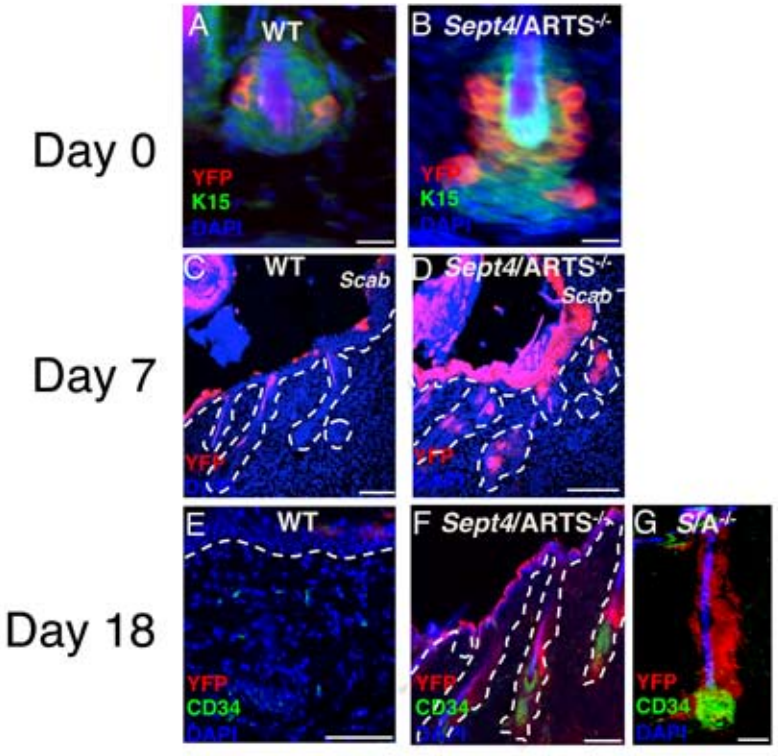

Figure S7. An increased number of YFP+ cells in the hair follicle and wounded epidermis of *Sept4*/ARTS$^{-/-}$ mice.

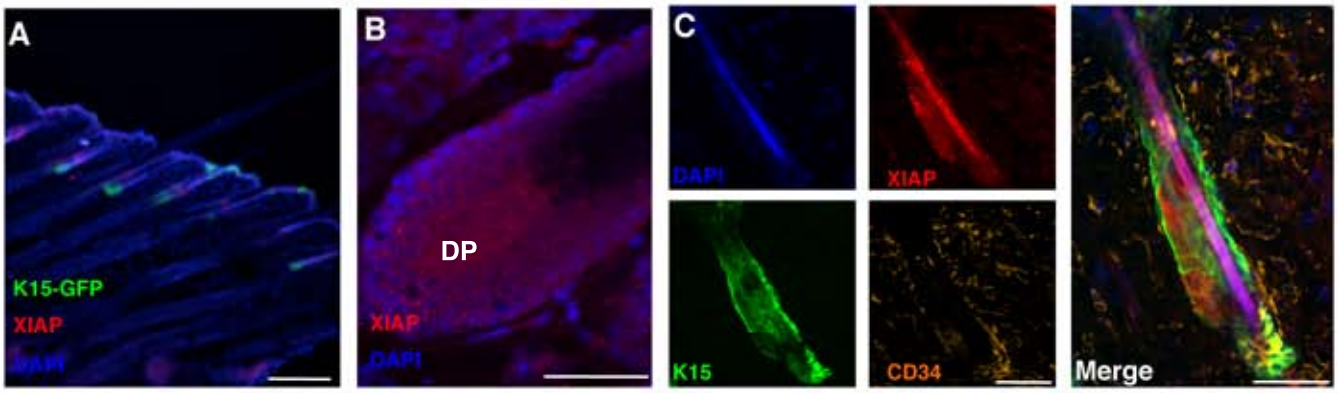

Figure S8. XIAP is expressed primarily in the HFSC niche, dermal papilla and sebaceous gland.

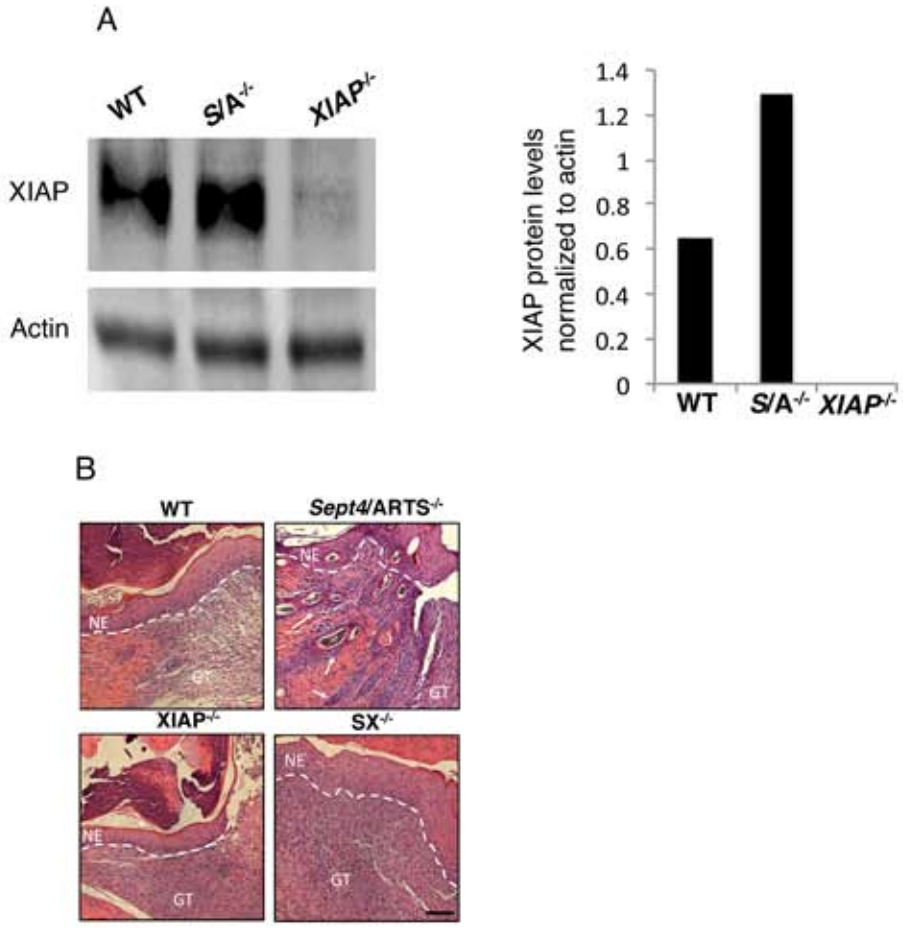

Figure S9. XIAP is regulated by and epistatic to *Sept4*/ARTS.

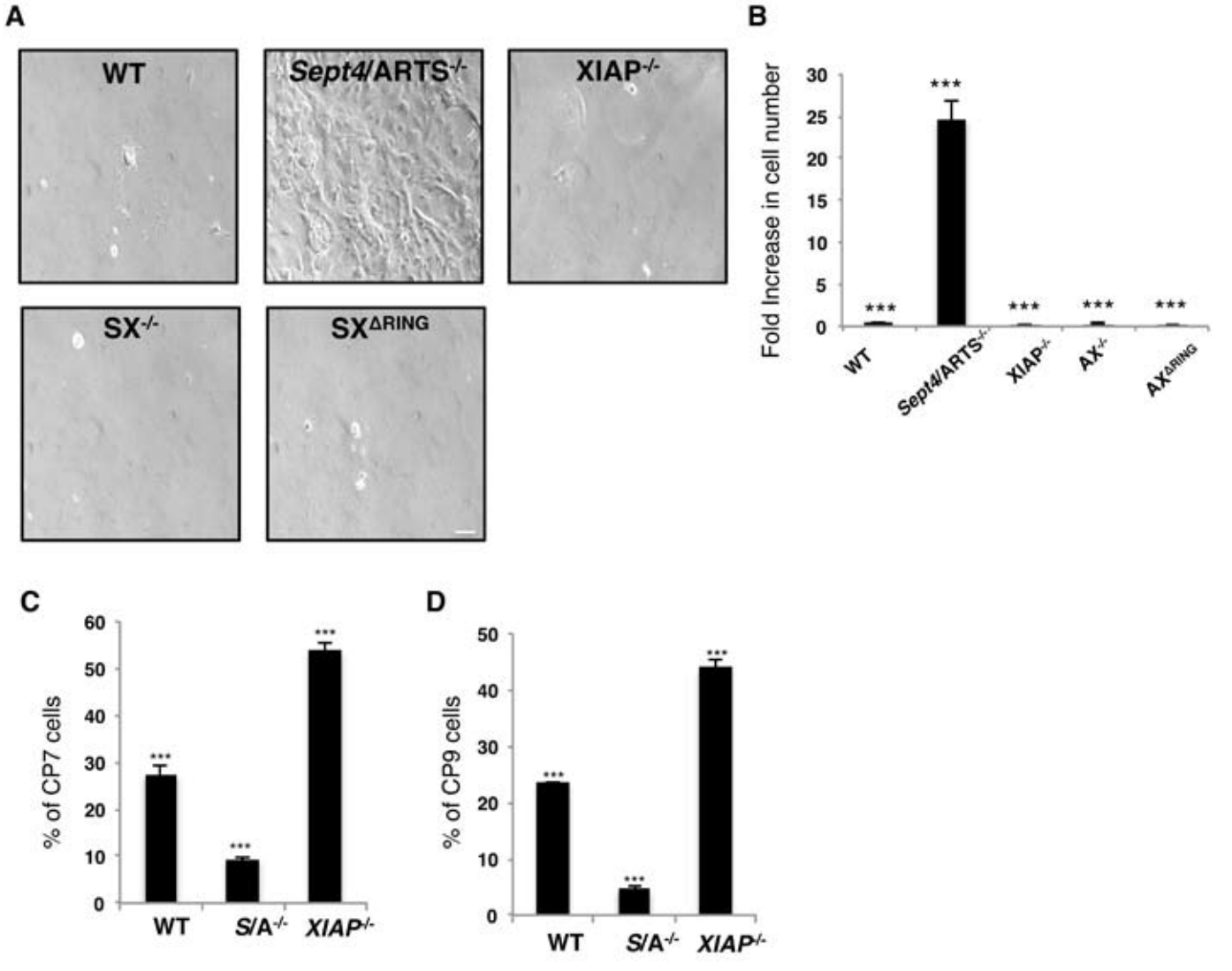

Figure S10. Deletion of XIAP suppresses *Sept4*/ARTS phenotypes in the skin and affects HFSC apoptosis.

References

1. I. L. Weissman, Translating stem and progenitor cell biology to the clinic: Barriers and opportunities. *Science* **287**, 1442–1446 (2000). doi:10.1126/science.287.5457.1442

2. S. Rafii, D. Lyden, Therapeutic stem and progenitor cell transplantation for organ vascularization and regeneration. *Nat. Med.* **9**, 702–712 (2003). doi:10.1038/nm0603-702 Medline

3. Y. C. Hsu, E. Fuchs, A family business: Stem cell progeny join the niche to regulate homeostasis. *Nat. Rev. Mol. Cell Biol.* **13**, 103–114 (2012). doi:10.1038/nrm3272 Medline

4. Y. Fuchs, H. Steller, Programmed cell death in animal development and disease. *Cell* **147**, 742–758 (2011). doi:10.1016/j.cell.2011.10.033 Medline

5. M. Gyrd-Hansen, P. Meier, IAPs: From caspase inhibitors to modulators of NF-κB, inflammation and cancer. *Nat. Rev. Cancer* **10**, 561–574 (2010). doi:10.1038/nrc2889 Medline

6. E. Kuranaga, M. Miura, Nonapoptotic functions of caspases: Caspases as regulatory molecules for immunity and cell-fate determination. *Trends Cell Biol.* **17**, 135–144 (2007). doi:10.1016/j.tcb.2007.01.001 Medline

7. A. J. Schile, M. García-Fernández, H. Steller, Regulation of apoptosis by XIAP ubiquitin-ligase activity. *Genes Dev.* **22**, 2256–2266 (2008). doi:10.1101/gad.1663108 Medline

8. S. Kornbluth, K. White, Apoptosis in *Drosophila*: Neither fish nor fowl (nor man, nor worm). *J. Cell Sci.* **118**, 1779–1787 (2005). doi:10.1242/jcs.02377 Medline

9. A. Bergmann, A. Y. Yang, M. Srivastava, Regulators of IAP function: Coming to grips with the grim reaper. *Curr. Opin. Cell Biol.* **15**, 717–724 (2003). doi:10.1016/j.ceb.2003.10.002 Medline

10. S. Larisch, Y. Yi, R. Lotan, H. Kerner, S. Eimerl, W. Tony Parks, Y. Gottfried, S. Birkey Reffey, M. P. de Caestecker, D. Danielpour, N. Book-Melamed, R. Timberg, C. S. Duckett, R. J. Lechleider, H. Steller, J. Orly, S. J. Kim, A. B. Roberts, A novel mitochondrial septin-like protein, ARTS, mediates apoptosis dependent on its P-loop motif. *Nat. Cell Biol.* **2**, 915–921 (2000). doi:10.1038/35046566 Medline

11. Y. Gottfried, A. Rotem, R. Lotan, H. Steller, S. Larisch, The mitochondrial ARTS protein promotes apoptosis through targeting XIAP. *EMBO J.* **23**, 1627–1635 (2004). doi:10.1038/sj.emboj.7600155 Medline

12. M. García-Fernández, H. Kissel, S. Brown, T. Gorenc, A. J. Schile, S. Rafii, S. Larisch, H. Steller, Sept4/ARTS is required for stem cell apoptosis and tumor suppression. *Genes Dev.* **24**, 2282–2293 (2010). doi:10.1101/gad.1970110 Medline

13. E. Fuchs, Scratching the surface of skin development. *Nature* **445**, 834–842 (2007). doi:10.1038/nature05659 Medline

14. S. J. Morrison, A. C. Spradling, Stem cells and niches: Mechanisms that promote stem cell maintenance throughout life. *Cell* **132**, 598–611 (2008). doi:10.1016/j.cell.2008.01.038 Medline

15. C. A. Jahoda, A. M. Christiano, Niche crosstalk: Intercellular signals at the hair follicle. *Cell* **146**, 678–681 (2011). doi:10.1016/j.cell.2011.08.020 Medline

16. W. M. Woo, A. E. Oro, Hair follicle stem cells. *Cell* **146**, 334 (2011). doi:10.1016/j.cell.2011.07.001

17. R. J. Morris, Y. Liu, L. Marles, Z. Yang, C. Trempus, S. Li, J. S. Lin, J. A. Sawicki, G. Cotsarelis, Capturing and profiling adult hair follicle stem cells. *Nat. Biotechnol.* **22**, 411–417 (2004). doi:10.1038/nbt950 Medline

18. Y. C. Hsu, H. A. Pasolli, E. Fuchs, Dynamics between stem cells, niche, and progeny in the hair follicle. *Cell* **144**, 92–105 (2011). doi:10.1016/j.cell.2010.11.049 Medline

19. S. Müller-Röver, B. Handjiski, C. van der Veen, S. Eichmüller, K. Foitzik, I. A. McKay, K. S. Stenn, R. Paus, A comprehensive guide for the accurate classification of murine hair follicles in distinct hair cycle stages. *J. Invest. Dermatol.* **117**, 3–15 (2001). doi:10.1046/j.0022-202x.2001.01377.x Medline

20. M. Ito, Y. Liu, Z. Yang, J. Nguyen, F. Liang, R. J. Morris, G. Cotsarelis, Stem cells in the hair follicle bulge contribute to wound repair but not to homeostasis of the epidermis. *Nat. Med.* **11**, 1351–1354 (2005). doi:10.1038/nm1328 Medline

21. I. Brownell, E. Guevara, C. B. Bai, C. A. Loomis, A. L. Joyner, Nerve-derived sonic hedgehog defines a niche for hair follicle stem cells capable of becoming epidermal stem cells. *Cell Stem Cell* **8**, 552–565 (2011). doi:10.1016/j.stem.2011.02.021 Medline

22. M. Ito, Z. Yang, T. Andl, C. Cui, N. Kim, S. E. Millar, G. Cotsarelis, Wnt-dependent de novo hair follicle regeneration in adult mouse skin after wounding. *Nature* **447**, 316–320 (2007). doi:10.1038/nature05766 Medline

23. J. C. Reed, Apoptosis-targeted therapies for cancer. *Cancer Cell* **3**, 17–22 (2003). doi:10.1016/S1535-6108(02)00241-6 Medline

24. E. C. LaCasse, D. J. Mahoney, H. H. Cheung, S. Plenchette, S. Baird, R. G. Korneluk, IAP-targeted therapies for cancer. *Oncogene* **27**, 6252–6275 (2008). doi:10.1038/onc.2008.302 Medline

25. H. Harlin, S. B. Reffey, C. S. Duckett, T. Lindsten, C. B. Thompson, Characterization of XIAP-deficient mice. *Mol. Cell. Biol.* **21**, 3604–3608 (2001). doi:10.1128/MCB.21.10.3604-3608.2001 Medline

26. W. H. Lien, X. Guo, L. Polak, L. N. Lawton, R. A. Young, D. Zheng, E. Fuchs, Genome-wide maps of histone modifications unwind in vivo chromatin states of the hair follicle lineage. *Cell Stem Cell* **9**, 219–232 (2011). doi:10.1016/j.stem.2011.07.015 Medline

27. J. B. Garrison, R. G. Correa, M. Gerlic, K. W. Yip, A. Krieg, C. M. Tamble, R. Shi, K. Welsh, S. Duggineni, Z. Huang, K. Ren, C. Du, J. C. Reed, ARTS and Siah collaborate in a pathway for XIAP degradation. *Mol. Cell* **41**, 107–116 (2011). doi:10.1016/j.molcel.2010.12.002 Medline

28. N. Edison, D. Zuri, I. Maniv, B. Bornstein, T. Lev, Y. Gottfried, S. Kemeny, M. Garcia-Fernandez, J. Kagan, S. Larisch, The IAP-antagonist ARTS initiates caspase activation upstream of cytochrome C and SMAC/Diablo. *Cell Death Differ.* **19**, 356–368 (2012). doi:10.1038/cdd.2011.112 Medline

29. S. Fulda, D. Vucic, Targeting IAP proteins for therapeutic intervention in cancer. *Nat. Rev. Drug Discov.* **11**, 109–124 (2012). doi:10.1038/nrd3627 Medline

30. F. Li, Q. Huang, J. Chen, Y. Peng, D. R. Roop, J. S. Bedford, C. Y. Li, Apoptotic cells activate the “phoenix rising” pathway to promote wound healing and tissue regeneration. *Sci. Signal.* **3**, ra13 (2010). doi:10.1126/scisignal.2000634 Medline

31. A. Bergmann, H. Steller, Apoptosis, stem cells, and tissue regeneration. *Sci. Signal.* **3**, re8 (2010). doi:10.1126/scisignal.3145re8 Medline

32. H. Kissel, M. M. Georgescu, S. Larisch, K. Manova, G. R. Hunnicutt, H. Steller, The Sept4 septin locus is required for sperm terminal differentiation in mice. *Dev. Cell* **8**, 353–364 (2005). doi:10.1016/j.devcel.2005.01.021 Medline

33. C. Blanpain, W. E. Lowry, A. Geoghegan, L. Polak, E. Fuchs, Self-renewal, multipotency, and the existence of two cell populations within an epithelial stem cell niche. *Cell* **118**, 635–648 (2004). doi:10.1016/j.cell.2004.08.012 Medline

34. C. P. Lu, L. Polak, A. S. Rocha, H. A. Pasolli, S. C. Chen, N. Sharma, C. Blanpain, E. Fuchs, Identification of stem cell populations in sweat glands and ducts reveals roles in homeostasis and wound repair. *Cell* **150**, 136–150 (2012). doi:10.1016/j.cell.2012.04.045 Medline

35. H. Fujiwara, M. Ferreira, G. Donati, D. K. Marciano, J. M. Linton, Y. Sato, A. Hartner, K. Sekiguchi, L. F. Reichardt, F. M. Watt, The basement membrane of hair follicle stem cells is a muscle cell niche. *Cell* **144**, 577–589 (2011). doi:10.1016/j.cell.2011.01.014 Medline